Progress In Electromagnetics Research M, Vol. 20, 57–71, 2011

DESIGN AND OPTIMIZATION OF A PERMANENT MAGNET ROTATING MACHINE FOR POWER COOLING GENERATION

H. R. E. H. Bouchekara[1, *], M. T. Simsim[1], Y. Berrouche[2], and M. Anwari[1]

[1]Department of Electrical Engineering, College of Engineering and Islamic Architecture, Umm Al-Qura University, P. O. Box 5555, Makkah 21955, Saudi Arabia

[2]Department of Electrical Engineering and Computer Engineering, Concordia University, 1455, De Maisonneuve Blvd. W., Montreal, Quebec H3G 1M8, Canada

Abstract—Magnetic refrigeration is an innovative, revolutionary, efficient and environmentally friendly cooling technology which is on the threshold of commercialization. The essential components of magnetic refrigeration system are the magnetic field generator and the magnetocaloric material. The two main goals of this paper are to design and to optimize a permanent magnet magnetic refrigeration machine for power cooling generation, where an initial configuration is studied and based on this study two other configurations are presented. Both electromagnetic and thermal studies are explored. The electromagnetic design part has been accomplished by using the finite elements method and the thermal design part has been achieved using the finite difference method.

1. INTRODUCTION

Nowadays, refrigeration is required in several areas e.g., food preservation, air conditioning, medical appliances, organ and tissue cryo-storage, cryo-surgery and aeronautic industry. Modern life style relies very much on readily available cooling. Magnetic refrigeration (MR) becomes a promising competitive technology to the conventional gas-compression/expansion [1, 2]. MR is a compact, reliable, and efficient technology since it doesn't require compressor

Received 27 June 2011, Accepted 8 August 2011, Scheduled 10 August 2011

* Corresponding author: H. R. El Hana Bouchekara (bouchekara.houssem@gmail.com).

(which is the most inefficient part in conventional refrigeration). The cycle efficiency of magnetic refrigeration can achieve 30% to 60% of Carnot cycle, which is much higher than conventional vapor compression refrigeration cycle, which generally achieves only 5%–10% of Carnot cycle [3]. Furthermore it is environmentally safe since only water and solid materials are used instead of the chlorofluorocarbon refrigerants that are usually used in the conventional refrigeration. The chlorofluorocarbon causes many damages such as toxicity, ozone depletion or global warming hazard [4].

The MR is based on the magneto-caloric effect (MCE) [1, 5]. The MCE was first discovered in iron compound by Warburg [1]. The MCE is defined as the response of a solid material to an applied magnetic field (generated with permanent magnet for instance), which is apparent as a change in its temperature (Fig. 1). When such solid materials are placed in a magnetic field, in what is called magnetization phase (Fig. 2), their temperature increases (i.e., they emit heat to the outside world) [4]. When the materials are removed from the magnetic field, they cool down (i.e., they absorb heat from the outside world) [4, 6]. This last phase is called demagnetization phase as shown in Fig. 2.

However, the temperature span generated by a cycle of magnetization demagnetization is limited to a couple of degrees, for

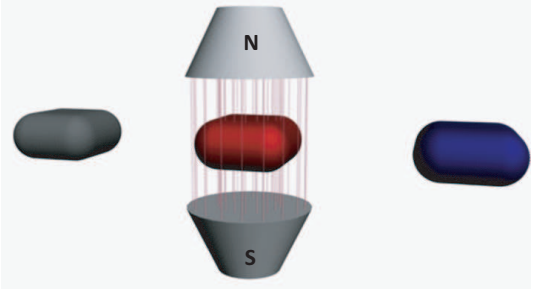

Figure 1. Illustration of the magnetocaloric effect.

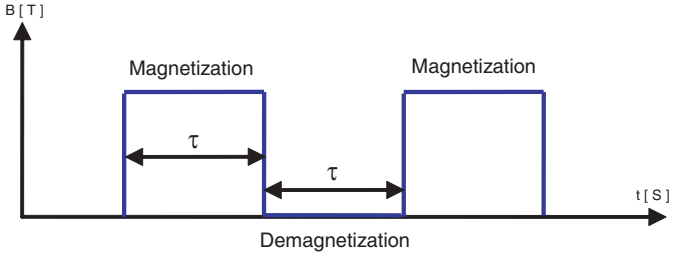

Figure 2. Cycles of magnetization and demagnetization phases.

instance near 2 K/T for gadolinium. Steyert has solved this limitation by proposing a special MR cycle, namely Active Magnetic Regenerative Refrigeration (AMRR), which leads to greater temperature span [7, 8]. AMRR is a refrigeration concept that uses the magnetocaloric effect (MCE) of a refrigerant bed and the thermal wave propagation regeneration aspect of an exchange fluid passing through the solid bed [4]. AMRR consists of four steps:

1) bed magnetization, warming the magnetic material and the bed fluid by the MCE;
2) cold to hot exchange fluid flow through the bed, transferring heat to one end of the bed;
3) bed demagnetization, cooling the magnetic material and exchange fluid; and
4) hot to cold flow through the bed, absorbing heat at the opposite end of the bed [2].

From the definition of MCE, it is clear that MR generator operates by submitting an MCE material to a varying magnetic field between a high level and a low level with $\Delta B = B_{\text{high}} - B_{\text{low}}$ as shown in Fig. 2. This paper presents the design and optimization of a rotating permanent magnet machine for cooling power generation by studying the influence of different factors on its performance using the classical parametric method and the statistical design of experiment method. Both electromagnetic and thermal studies are performed. Electromagnetic computations are undertaken to maximize the ΔB in order to get the best MR performance (temperature span and cooling power) and to limit mechanical efforts (forces and torque). Furthermore, the conducted thermal study aims to evaluate the cooling performance of such machines.

2. CONFIGURATION AND WORKING PRINCIPLE

The initial configuration is similar to the one used in [6, 7]. This structure is quite similar to a rotating synchronous machine as shown in Fig. 3. The stator of this machine consists of a cylindrical yoke and two pairs of containers called beds (b_1, b_2, b_3 and b_4) filled with MCE materials (for instance Gadolinium). The beds are placed around a rotating magnet (rotor). The yoke has two major roles; the first one is to canalize the magnetic flux (to close the magnetic flux path within the refrigerant bed) and the second one is to support the containers. The rotation of the permanent magnet (PM) will generate cycles of varying magnetic field between B_{high} and B_{low}. The beds undergo an AMRR cycle and operate two by two in an opposite way; i.e., that

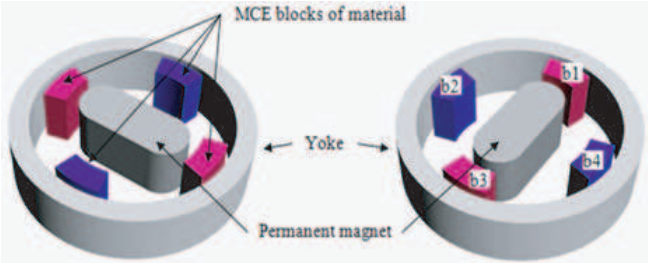

Figure 3. Configuration and working principle of the PM cooling machine.

when b_1 and b_3 are magnetized b_2 and b_4 are demagnetized and vice versa.

The regenerator (MCE block) itself can be either plates or a packed bed of magnetocaloric material. The performance of the refrigeration system depends on many parameters such as: the dimensions of the shape, the stacking of the plates and the dimensions of the packed bed.

3. DESIGN

3.1. Electromagnetic Design

The electromagnetic study is achieved by simulating the system using the finite element method (FEM). Since 3D FEM is computationally expensive and time consuming for the design optimization of such machines, investigations were performed in 2D. This can be justified by the longitudinal symmetry of the geometry (there is no change of the geometry along the vertical axis). Moreover, due to the length of the machine, the end effects of the machine do not have such an influence on the total performance. The problem has been solved in magnetostatic formulation. Rotor motion is easily modeled due to the parameterization of its angular position (called α). The electromagnetic study is undertaken to compute the profiles of the variation of magnetic field, torque and forces.

In these studies, the remanent magnetization and the relative permeability of the magnet are fixed respectively to $1.46T$ and 1.046 (NdFeB magnets). The stator is described by a constant permeability equals to 1000 and the MCE material by an isotropic bulk gadolinium material with a relative permeability of 5.

Based on numerical modeling of the AMRR process using the model developed in [6] and [9] (which will be detailed in the thermal

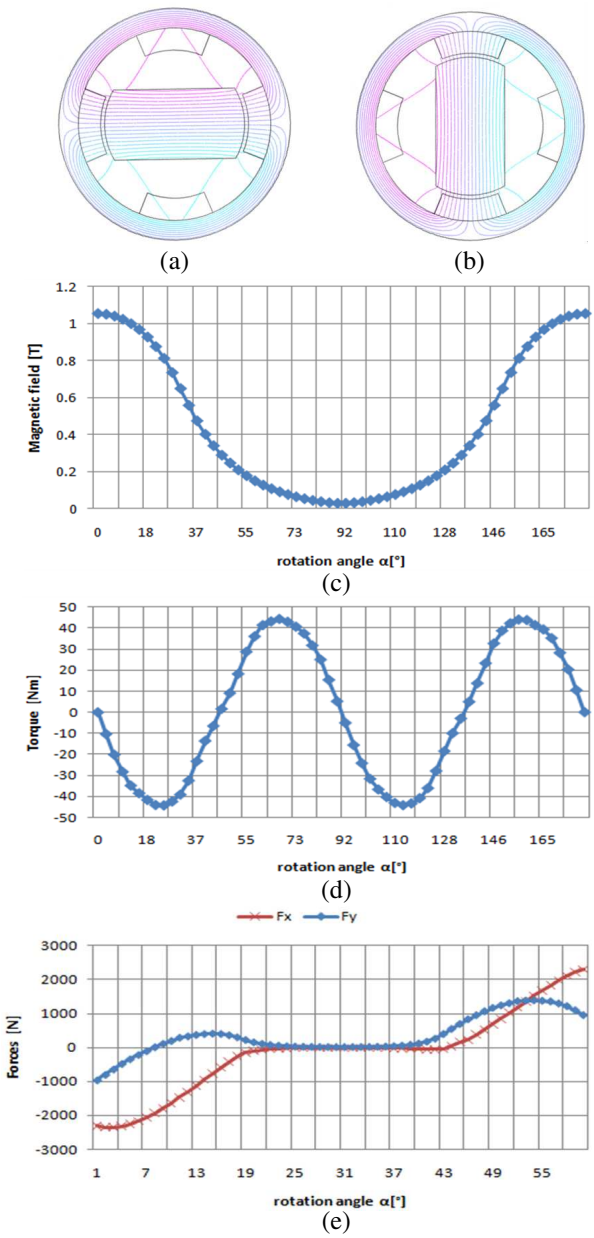

Figure 4. Electromagnetic modeling of the initial configuration. (a) Magnetic card obtained for the position $\alpha = 0°$. (b) Magnetic card obtained for the position $\alpha = 90°$. (c), (d) and (e) are respectively, the profiles of the magnetic field, the torque and the magnetic forces versus α.

study section) the length L of the structure is chosen to be 100 mm. The external radius R_e of the stator is equal to 88.5 mm and an internal radius R_i of 73.5 mm is chosen. The radius and the angular size of the rotor are chosen respectively as $R_r = 53.5$ mm and $a_r = 60°$. The angular size and the width of the MCE blocks are chosen to be $a_b = 45°$ and $w_b = 17$ mm, respectively.

Figure 4(a) gives the magnetic flux cards obtained for 2 different positions given by $\alpha = 0°$ and $\alpha = 90°$. For $\alpha = 0°$, the MCE blocks (or beds) b_1 and b_3 are submitted to the magnetic field created by magnets. Consequently they are magnetized. Inversely, the beds b_2 and b_4 are not submitted to the magnetic field and they undergo the demagnetization phase. Now if the magnet is rotated by $\alpha = 90°$ beds b_1 and b_3 are no longer submitted to the magnetic field thus, they are demagnetized while beds b_2 and b_4 are now magnetized. So, the cycles of the magnetic field crated into the beds have a period of 180° as shown in Fig. 4(c).

Figures 4(d) and (e) show the sketch of the magnetic efforts respectively the torque (on the rotor) and the forces (on one bed). The total torque and the total forces can be seen as the result of the action of the magnet (rotor) on the MCE blocks of the stator. The torque is of course deduced from the force by its multiplication by the radius of the device.

3.2. Thermal Design

Governing equations for AMRR system have been developed in [6] and [7]. The heat exchanges between the fluid and the MCE regenerator is described by the following equations (in 1 dimension):

$$\begin{cases} m_f C_f \left(\dfrac{\partial T_{f(t,x)}}{\partial t} + \mathbf{V} \dfrac{\partial T_{f(t,x)}}{\partial x} \right) = hS \left(T_{m(t,x)} - T_{f(t,x)} \right) \\ m_m C_m \left(\dfrac{\partial T_{m(t,x)}}{\partial t} \right) = hS \left(T_{f(t,x)} - T_{m(t,x)} \right) \\ Q_{(t,x)} = h \left(T_{m(t,x)} - T_{f(t,x)} \right) St \end{cases} \tag{1}$$

where: T is the temperature, Q is the energy, C is the specific heat of either fluid or material, m is the mass, the indexes f and m are related to the fluid and the material respectively, $\mathbf{V}$ is the fluid velocity, S is the cross sectional area of the regenerator bed, h is the convection heat transfer coefficient and t is the time.

To solve this system the finite difference method is used. A right difference is used to approximate time derivatives and a left difference is used to approximate space derivatives. Thus, a central scheme is obtained.

After some manipulation/simplification the final system of equations is given by:

$$\begin{cases} T_{f(i+1,j)} = A_{f1}T_{f(i,j)} + A_{f2}T_{f(i,j-1)} + A_{f3}T_{m(i,j)} \\ T_{m(i+1,j)} = A_{m1}T_{m(i,j)} + A_{m2}T_{f(i,j)} \\ q_{(i+1,j)} = hS\left(T_{m(i+1,j)} - T_{f(i+1,j)}\right) \end{cases} \quad (2)$$

where: $A_{f1} = (1 - (V\frac{\Delta t}{\Delta x} + \frac{hS}{m_f C_f}\Delta t))$, $A_{f2} = (V\frac{\Delta t}{\Delta x})$, $A_{f3} = (\frac{h \cdot S}{m_f C_f}\Delta t)$, $A_{m1} = (1 - \frac{h \cdot S}{m_m C_m}\Delta t)$ and $A_{m2} = (\frac{h \cdot S}{m_m \cdot C_m}\Delta t)$

The thermal model has been implemented under Matlab. This model is explained in details in [6]. The main results of the thermal design are displayed in Fig. 5.

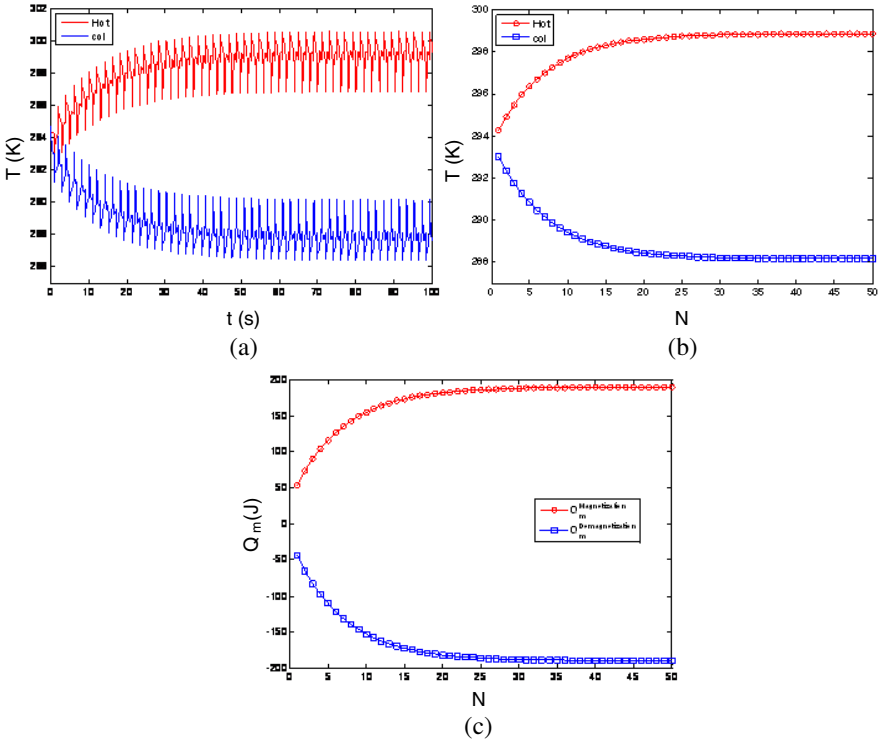

Figure 5. Main results obtained by the developed model. (a) Temperature profile of hot and cold sides over the time. (b) Temperature profile of hot and cold sides at the end of each AMRR cycle where N represent the number of cycles. (c) Profile of the energy exchanged between the material and the fluid.

The gradient of temperature created within the material, i.e., between the cold and the hot sides, is due to the AMRR cycles as explained in Section 1. Fig. 5(a) shows the evolution of the temperature for both sides (hot and cold) of the material over time. The fluctuations in this curve are due to the 4 steps (previously described) of the AMRR. After a transitional period the two curves reach their steady state. By using the AMRR the obtained temperature span ΔT (between the cold and the hot ends) at the steady state is higher than the initial EMC as expected ($\Delta T = 11\,\mathrm{K}$). The evolution of temperature at the end of each cycle (one cycle consists of 4 steps), is shown for both sides in Fig. 5(b). The slight difference between the two curves shown in this figure is due only to a programming choice, because the phase of magnetization is programmed as the first step before the demagnetization phase.

In addition to temperature profiles, the developed thermal model allows to obtain profiles of the energy exchanged between the fluid and material during the AMRR cycles.The energy exchanged by convection between the magnetocaloric material and the fluid is decomposed into two parts: the one exchanged during the magnetization and the one exchanged during the demagnetization. The profile of the evolution of energy is shown in Fig. 5(c).

4. NEAR-OPTIMAL ANALYSIS

4.1. Objective Function

Since the magneto-caloric effect depends on the magnitude of the magnetic field, the performance of the machine is directly related to the magnetic field range ΔB. Thus, the ΔB should be the first criterion to be taken into account for the design and the optimization process. The objective for this criterion is to maximize the ΔB. The second criterion should be the minimization of the magnetic efforts (Forces and Torque). The third and last criterion is the thermal behavior, i.e., the generated temperature span ΔT and the produced cooling power (Pc). The objective for this last criterion is to maximize both the temperature span and the generated cooling power.

The objective function for the optimization process is given by:

$$F_{\text{objective}} = \{f_1, f_2, f_3, f_4, f_5\} \tag{3}$$

where

$$f_1 = \max(\Delta B) \tag{4}$$

$$f_2 = \min(\text{Forces}) \tag{5}$$

$$f_3 = \min(\text{Torque}) \tag{6}$$

$$f_4 = \max(\Delta T) \tag{7}$$

$$f_5 = \max(Pc) \tag{8}$$

Several optimization methods can solve (3) using a large number of calculations of the objective function. Using the finite element model (FEM) for the electromagnetic study and the finite difference (FDM) for the thermal study with traditional methods of optimization, will require a huge number of evaluations of the objective function [10, 11].

While there are potentially many parameters (factors) that affect the performance of the machine (objective function), some parameters are more important, *viz*, have a greater impact on the objective. Statistically designed experiments method (DOE) provide a systematic & efficient plan of experimentation or simulation to compute the effect of factors on the performance of the machine, so that several factors can be studied simultaneously [10, 12]. The DOE is an effective tool for maximizing the amount of information obtained from a study while minimizing the amount of data to be collected, which is in this case, is minimizing the number of simulation runs [13].

Instead of conducting many separate studies by varying one factor at a time (using classical methods), factorial designs investigate the cause and the effects of several factors in only one single study. There is another advantage of using DOE techniques, factorial designs allow estimation of the influence of each factor and also their interactions (combinations; two by two, three by three, ..., n by n). Nonetheless, using the classical methods (varying one factor at a time and keeping the other factors constant) will not give any indications of the interactions [9]. In some cases when the influence of a large number of factors is to be investigated it is obvious that the number of combinations will increase geometrically. In these cases, studies employing DOE method should use a method such as the Fractional Factorial designs rather than full factorial designs. Fractional factorial designs produce high confidence in sensitivity results using less number of runs [6, 10, 13, 14].

4.2. Fractional 2 Levels Factorial Design

Here, the DOE is applied to analyze the objective function. The proposed approach uses tools of the experimental design method: fractional designs, notably of G. Box Generators to estimate the performance of the power cooling machine. The interest is to save calculation time and to find a near global optimum. The saving of time

Table 1. Considered parameters.

Name	Description	Initial Value	Minimum Value	Maximum Value	Type
L	Length of the machine	100 mm	90 mm	110 mm	Continuous
R_e	External radius of the yoke	88.5 mm	80.5 mm	99.5 mm	Continuous
R_i	Internal radius of the yoke	73.5 mm	73.5 mm	77.5 mm	Continuous
R_r	Radius of the rotor	53.5 mm	47.5 mm	53.5 mm	Continuous
a_r	Angular size of the rotor	60°	45°	60°	Continuous
a_b	Angular size of the magnetocaloric material Blocks	45°	30°	45°	Continuous
w_b	Width of the magnetocaloric material Blocks	17 mm	10 mm	17 mm	Continuous
N_b	Number of the magnetocaloric material Blocks	4	2	6	Discreet

can be substantial because the number of FEM and FDM simulations needed is significantly reduced.

Since eight parameters define the shape of the machine, it is advisable to determine the effect of each parameter on the objective function. Thus, it is very important to provide proper parameter ranges. The considered parameters are listed in Table 1. There are two types of parameters; continuous parameters (they can take any value inside the defined range like the length of the machine, the radius of the rotor, etc.) and discrete parameters (since a 2 level design is used so they can take only the limits of the defined range like the number of blocks).

4.3. Results

Using two-level full factorial design needs $2^8 = 256$ runs (simulations) to evaluate the objective function. Using a 2^{8-4} fractional factorial design will significantly reduce the number of runs from 256 to 16. The 2^{8-4} design is given using Generators of G. Box as shown in Table 2. The choice of a 2^{8-4} means that we have a 2 levels design with 8 factors where 4 of these factors are generated using the other 4 factors as shown in the appendix (Table A1). Thus:

- √ The factor (5) will be generated using the product of factors (2), (3) and (4).
- √ The factor (6) will be generated using the product of factors (1),

Table 2. Design matrix generated by the 2^{8-4} Box-Wilson fractional factorial design and the simulation results.

N °	L [mm]	R_e [mm]	R_i [mm]	R_r [mm]	a_r [°]	a_b [°]	w_b [mm]	N_b	ΔB [T]	Torque [N.m]	Forces [N]	ΔT [K]	Pc [W]
1	90	85.5	73.5	47.5	45	30	10	2	0.56579	8.3397	-124.95	2.7	106
2	90	85.5	73.5	53.5	60	45	10	6	0.81441	4.0532	-532.66	11.4	441
3	90	85.5	77.5	47.5	60	45	17	2	0.61438	19.4440	-354.97	6.4	273
4	90	85.5	77.5	53.5	45	30	17	6	0.85772	16.5120	-290.60	12.7	488
5	90	99.5	73.5	47.5	60	30	17	6	0.85831	6.1528	-266.31	12.4	476
6	90	99.5	73.5	53.5	45	45	17	2	0.91797	40.4441	-645.45	9.3	370
7	90	99.5	77.5	47.5	45	45	10	6	0.44317	2.0692	-154.36	6.4	270
8	90	99.5	77.5	53.5	60	30	10	2	0.77045	16.5523	-253.22	4.0	156
9	110	85.5	73.5	47.5	45	45	17	6	0.63619	6.1388	-375.38	12.1	509
10	110	85.5	73.5	53.5	60	30	17	2	1.17272	55.1549	-617.04	10.9	434
11	110	85.5	77.5	47.5	60	30	10	6	0.55053	3.1761	-163.76	7.6	390
12	110	85.5	77.5	53.5	45	45	10	2	0.61404	16.9514	-363.43	5.7	253
13	110	99.5	73.5	47.5	60	45	10	2	0.60799	14.7476	-372.99	5.4	244
14	110	99.5	73.5	53.5	45	30	10	6	0.80641	14.1823	-293.53	10.9	460
15	110	99.5	77.5	47.5	45	30	17	2	0.61751	16.7636	-181.47	6.0	282
16	110	99.5	77.5	53.5	60	45	17	6	0.85549	5.8050	-749.81	16.6	693

Table 3. Contrasts and contribution obtained.

Contrasts	ΔB	Significant?	Torque	Significant?	Forces	Significant?	ΔT	Significant?	Pc	Significant?
L	0	No	1	No	3	No	3	No	9	Yes
R_e	0	No	0	No	0	No	0	No	0	No
R_i	14	Yes	6	Yes	6	Yes	3	No	1	No
R_r	46	Yes	18	Yes	36	Yes	14	Yes	10	Yes
a_r	8	Yes	0	No	9	Yes	2	No	2	No
a_b	6	Yes	2	No	22	Yes	1	No	1	No
w_b	23	Yes	16	Yes	18	Yes	30	Yes	27	Yes
N_b	0	No	35	Yes	0	No	45	Yes	48	Yes
$L\times R_e+R_i\times w_b+R_r\times N_b+a_r\times a_b$	1	No	5	Yes	0	No	0	No	0	No
$L\times R_i+R_r\times a_b+R_e\times w_b+a_r\times N_b$	0	No	4	No	1	No	0	No	1	No
$L\times R_r+R_i\times a_b+R_e\times N_b+a_r\times w_b$	0	No	0	No	0	No	0	No	0	No
$L\times a_r+R_e\times a_b+R_r\times w_b+R_i\times N_b$	1	No	4	No	3	No	0	No	0	No
$L\times a_b+R_i\times R_r+R_e\times a_r+w_b\times N_b$	0	No	9	Yes	0	No	0	No	0	No
$L\times w_b+R_e\times R_i+R_r\times a_r+a_b\times N_b$	0	No	1	No	1	No	0	No	0	No
$L\times N_b+R_e\times R_r+R_i\times a_r+a_b\times w_b$	1	No	1	No	0	No	0	No	0	No

(3) and (4).

√ The factor (7) will be generated using the product of factors (1), (2) and (3).

√ The factor (8) will be generated using the product of factors (1), (2) and (4).

The results obtained when the procedure described above is run for the power cooling machine are given in Table 2 and Table 3. Table 2 gives the design matrix generated by the 2^{8-4} Box-Wilson fractional factorial design and the simulation results obtained for this design. The contributions of obtained contrasts are given in Table 3. It shows in its first column contrasts and in the other columns their contribution or influences on the objective function. Keep in mind that a contribution is significant if it is higher than 5% and high order interactions (higher than 2) are considered negligible while only interactions of significant parameters are also significant.

The complicated multiple-objective function has been successfully converted into a simple and practical single-objective function using (9).

$$F_{\text{objective}} = \frac{1}{\sum_{i=1}^{5}(f_{i\text{Normalized}})^2} \tag{9}$$

However, since the 5 functions of the multi-objective function have different ranges, for instance $f_1 = \Delta B$ varies from 0.44 to 1.17 and

Table 4. Normalization of the objective functions.

N°	L	R_e	R_i	R_r	a_r	a_b	w_b	N_b	f_1	f_2	f_3	f_4	f_5	$F_{objective}$	Ranking
1	90	85.5	73.5	47.5	45	30	10	2	0.168077	0.21881	1	0	0	0.41	9
2	90	85.5	73.5	53.5	60	45	10	6	0.508862	0.49145	0.08152	0.62662	0.5705	0.57	7
3	90	85.5	77.5	47.5	60	45	17	2	0.234689	0.07159	0.22242	0.26861	0.28411	0.60	14
4	90	85.5	77.5	53.5	45	30	17	6	0.568223	0.09122	0.31599	0.72149	0.65062	0.70	5
5	90	99.5	73.5	47.5	60	30	17	6	0.569042	0.31044	0.36305	0.69914	0.63058	0.73	4
6	90	99.5	73.5	53.5	45	45	17	2	0.650814	0.01418	0.03233	0.47431	0.44998	0.77	11
7	90	99.5	77.5	47.5	45	45	10	6	0	1	0.77138	0.26239	0.27999	0.82	2
8	90	99.5	77.5	53.5	60	30	10	2	0.448604	0.09091	0.39214	0.0884	0.08503	0.88	13
9	110	85.5	73.5	47.5	45	45	17	6	0.264582	0.31123	0.19946	0.67779	0.68698	0.93	8
10	110	85.5	73.5	53.5	60	30	17	2	1	0	0.04303	0.59358	0.55915	0.94	3
11	110	85.5	77.5	47.5	60	30	10	6	0.147168	0.63792	0.71561	0.35389	0.48297	1.17	6
12	110	85.5	77.5	53.5	45	45	10	2	0.234218	0.08785	0.21258	0.21231	0.24987	1.66	15
13	110	99.5	73.5	47.5	60	45	10	2	0.225919	0.1068	0.20201	0.19243	0.23536	2.64	16
14	110	99.5	73.5	53.5	45	30	10	6	0.497901	0.11261	0.31084	0.58839	0.60396	3.81	10
15	110	99.5	77.5	47.5	45	30	17	2	0.238973	0.08927	0.62625	0.23833	0.29953	4.65	12
16	110	99.5	77.5	53.5	60	45	17	6	0.565178	0.33137	0	1	1	5.11	1

$f_5 = Pc$ varies from 106 to 693. Thus, the values of these functions are normalized from 0 to 1. Now, the minimum of all functions is equal to 0 and the maximum is equal to 1 using the following expression:

$$\text{Normalized}_{\text{Value}} = \frac{(\text{Actual}_{\text{Value}} - \min(f_i))}{\max(f_i) - \min(f_i)} \tag{10}$$

Table 4 shows normalization of the multiple-objective function, the value of the new single-objective function and the ranking of the set of parameters giving the best compromises.

The optimal parameter set can be definitely chosen from Table 4 which is the sixtieth's set. Nonetheless, it is important here to mention that other set of parameters can be chosen depending on the constraints and the needs of the design engineer. If the need is to build the most performing prototype, then it is obvious that the parameter set to be chosen is number 16 (ranking 1). However, if the prototype to be built is a test prototype for new materials where less magnetic efforts are required, then the parameter set number 7 (ranking 2) can be chosen and so on.

5. CONCLUSION

The design and optimization of a permanent magnet rotating machine for power cooling generation has been presented. Both the magnetic design (using the finite element method) and the thermal design (using the finite difference method) have been investigated. The results of the magnetic design can be used to evaluate the magnetic field strength obtained by the permanent magnet structure and applied to the magnetocaloric material, the magnetic efforts on the rotor (torque) and on the magnetocaloric material blocks (forces). The thermal design results can be used to compute the temperature span and the cooling power generated by the machine.

The structure of the power cooling machine is optimized by minimizing a multi-objective function using the design of experiments technique. This technique is also used to identify the influence of each parameter on the objective function and whether each parameter has a significant influence or not. In an optimization study, only 16 sets of simulation cases were needed to obtain the satisfactory near-optimal parameter set and multiple sets of good results. When it comes to building the machine in the context of a practical magnetic refrigerator, the engineer has to choose from different set of parameters.

APPENDIX A.

Table A1. Generators of G. Box for 8 factors.

Resolution	Design name	Number of tests	Generators
4	2^{8-4}	16	5 = ± 2,3,4 6 = ± 1,3,4 7 = ± 1,2,3 8 = ± 1,2,4
4	2^{8-3}	32	6 = ± 1,2,3 7 = ± 1,2,4 8 = ± 2,3,4,5
5	2^{8-2}	64	7 = ± 1,2,3,4 8 = ± 1,2,5,6

REFERENCES

1. Hong, S. C., S. J. Kim, E. J. Hahn, S. Park, and C. S. Kim, "Magnetic refrigeration properties of $La_{0.8}Ca_{0.2}Mn^{57}_{0.99}Fe_{0.01}O_3$," *IEEE Transactions on Magnetics*, Vol. 45, No. 6, 2565–2568, Jun. 2009.
2. Bruck, E., O. Tegus, X. W. Li, et al., "Magnetic refrigeration-towards room-temperature applications," *Physica B: Condensed. Matter*, Vol. 327, No. 2–4, 431–437, Apr. 2003.
3. Han, L., X. Li, and D. Xia, "Design and experiment of a rotary room temperature permanent magnet refrigerator," *IEEE Transactions on Applied Superconductivity*, Vol. 20, No. 3, 870–873, Jun. 2010.
4. Shir, F., E. D. Torre, L. H. Bennett, et al., "Modeling of magnetization and demagnetization in magnetic regenerative refrigeration," *IEEE Transaction on Magnetics*, Vol. 40, No. 4, 2098–2100, Jul. 2004.
5. Dong, A. and X. Lu, "A new permanent magnet system for rotating magnetic refrigerator," *IEEE Transactions on Applied Superconductivity*, Vol. 20, No. 3, 834–837, Jun. 2010.
6. Bouchekara, H., "Recherche sur les systèmes de réfrigération magnétique," Modélisation Numérique, Conception et Optimisa-

tion, Ph.D. Thesis, National Polytechnic Institute of Grenoble, 2008.

7. Dupuis, C., "Matériaux à effet magnétocalorique géant et systèmes de réfrigération magnétique," Thèse de Doctorat, Ph.D. Thesis, National Polytechnic Institute of Grenoble, 2009.
8. Barclay, J. A. and W. A. Steyert, "Active magnetic regenerator," US Patent 4,332,135, 1982.
9. Bouchekara, H., A. Kedous-Lebouc, C. Dupuis, and F. Allab, "Prediction and optimisation of geometrical properties of the refrigerant bed in an AMRR cycle," *International Journal of Refrigeration*, Vol. 31, No. 7, 1224–1230, 2008.
10. Brisset, S., F. Gillon, S. Vivier, and P. Brochet, "Optimization with experimental design: An approach using Taguchi's methodology and finite element simulations," *IEEE Transactions on Magnetics*, Vol. 37, No. 5, 3530–3533, Sep. 2001.
11. Wang, Y. L., P. K. Liu, J. Wu, and H. Ding, "Near-optimal design and 3-D finite element analysis of multiple sets of radial magnetic couplings," *IEEE Transactions on Magnetics*, Vol. 44, No. 12, 4747–4753, Dec. 2008.
12. Bouchekara, H., G. Dahman, and M. Nahas, "Smart electromagnetic simulations: Guide lines for design of experiments technique," *Progress In Electromagnetics Research B*, Vol. 31, 357–379, 2011.
13. Bouchekara, H. and M. T. Simsim, "Design of a linear magnetic refrigeration structure running with rotating bar-shaped magnets," *14th Biennial IEEE Conference on Electromagnetic Field Computation (CEFC)*, 1–1, May 9–12, 2010.
14. Hamada, M., "Using statistically designed experiments to improve reliability and to achieve robust reliability," *IEEE Transactions on Reliability*, Vol. 44, No. 2, 206–215, Jun. 1995.